Polish Society of Composite Materials
Polskie Towarzystwo Materiałów Kompozytowych

16: 2 (2016) 113-121

COMPOSITES THEORY AND PRACTICE

Marian Klasztorny[1]*, Daniel B. Nycz[2]

[1]Military University of Technology, ul. gen. S. Kaliskiego 2, 00-908 Warsaw, Poland
[2]Jan Grodek State Vocational High School, ul. A. Mickiewicza 21, 38-500 Sanok, Poland
**Corresponding author. E-mail: m.klasztorny@gmail.com*

Received (Otrzymano) 29.03.2016

INFLUENCE OF TEMPERATURE AND AGEING ON LOAD CAPACITY OF GLASS-VINYLESTER BOX BEAM

The paper concerns the numerical testing of a GFRP composite box beam reflecting, on a 1:2 scale, the central part of the superstructure of the recently designed original GFRP composite 5-box footbridge manufactured using infusion technology. The beam is composed of two laminate shells combined with glue on contact strips. The shells are glass-vinyl ester laminates protected with gelcoat and topcoat layers, respectively. The main constituents of the laminas are bi-directional balanced stitched E-glass woven fabrics and flame retardant vinyl ester resin. After homogenization, the composite forming a lamina (reinforced with one fabric) is modelled as a linearly elastic-brittle orthotropic material. Experimental identification of the material constants was done for the new composite and for the aged composite after 5-year environmental ageing, at three service temperatures, i.e. –20, 20, 55°C. The accelerated 5-year environmental ageing of the composite was performed using an ageing chamber and the relevant ageing programme. The study presents the numerical modelling and simulation of the static three-point bending test of the new and aged box beam, at the three service temperatures. The modelling and simulation, performed in the MSC.Marc system, was validated in a previous paper by the authors, based on the experimental three-point bending test of the new beam at room temperature. Comparative studies were carried out in order to determine the effects of the service temperatures and the 5-year environmental ageing on the load capacity of the GFRP composite box beam.

Keywords: **glass-vinylester composite, mechanical properties, GFRP composite box beam, three-point bending test, modelling and simulation, temperature and ageing effects**

WPŁYW TEMPERATURY I STARZENIA NA NOŚNOŚĆ BELKI SKRZYNKOWEJ WINYLOESTROWO-SZKLANEJ

Praca dotyczy badań numerycznych kompozytowej belki skrzynkowej odwzorowującej w skali 1:2 centralną część konstrukcji nośnej ostatnio zaprojektowanej kładki pieszo-rowerowej o przekroju skrzynkowym. Konstrukcja nośna kładki składa się z dwóch powłok laminatowych sklejonych ze sobą na płaskich pasach kontaktu. Powłoki winyloestrowo-szklane, zabezpieczone warstwami ochronnymi (żelkot i topkot), wytworzono w technologii infuzji. Głównymi komponentami lamin są: tkanina szklana E dwukierunkowa zrównoważona zszywana oraz żywica winyloestrowa uniepalniona. Po homogenizacji, lamina (wzmocniona pojedynczą tkaniną) jest modelowana jako materiał ortotropowy liniowo sprężysto-kruchy. Stałe sprężystości i wytrzymałości kompozytu wyznaczono dla materiału nowego oraz materiału starzonego (przyspieszone starzenie 5-letnie), dla trzech poziomów temperatury użytkowania kładki, tj. –20, 20, 55°C. Starzenie przeprowadzono w komorze starzeniowej według odpowiednio dobranego programu starzenia. W pracy przedstawiono modelowanie numeryczne i symulację próby statycznego zginania trójpunktowego belki skrzynkowej nowej i poddanej starzeniu 5-letniemu dla trzech poziomów temperatury użytkowania kładki. Modelowanie i symulacja zostały wykonane w środowisku MSC.Marc i poddane walidacji w poprzedniej pracy autorów, w przypadku belki nowej w temperaturze pokojowej. Badania porównawcze dotyczą wpływu temperatury użytkowania i pięcioletniego starzenia na nośność kompozytowej belki skrzynkowej.

Słowa kluczowe: **kompozyt winyloestrowo-szklany, własności mechaniczne, belka skrzynkowa kompozytowa, test zginania trójpunktowego, modelowanie i symulacja, wpływ temperatury i starzenia**

INTRODUCTION

GFRP (glass fibre reinforced plastics) composite structures in civil engineering have some favourable characteristics such as high specific strength and stiffness, high resistance to fatigue, moisture, corrosion, and UV radiation, as well as relatively low material and maintenance costs. Recently, two innovative GFRP composite footbridges have been designed and manufactured using infusion technology [1, 2]. With regard to the footbridge designed in [2], the main constituents of the laminas are: (a) bi-directional balanced stitched E-glass woven fabrics of an 800 gsm surface mass, with [0/90] and [45/–45] orientation with respect to the footbridge longitudinal axis, used as the reinforcement, (b) flame retardant vinyl ester resin used as the matrix.

The design criteria for civil engineering GFRP composite structures should take into consideration the following factors: (a) spatial complex stress states in laminas with specified orientations, (b) a commonly recognized approximate linearly elastic-brittle orthotropic homogenised model of laminas, (c) relatively low shear moduli and shear strengths of laminas, (d) dependence of the lamina mechanical characteristics on the components, laminate manufacturing technology, additives, protective layers, chemical resistance class, heat deflection temperature (HDT) of the resin, design/service temperature range, environmental ageing, (e) load types, and (f) durability.

A given composite structure has assigned, among others, the service temperature range to which it may be exposed, and the durability. The design of composite structures is mostly based on design coefficients (safety coefficients), e.g. as for composite tanks and pressure vessels [3]. Of key importance in the design of civil engineering composite structures are: the choice of composite material model in reference to each lamina and identification of the material constants of each composite used in the superstructure. The safety factors should take into account, among others, the impact of environmental ageing and service temperature on the load capacity, stability, deflections and dynamic characteristics of the designed structure. The polymer matrix in GFRP composites can be in glassy, leathery, rubbery or decomposed states depending on the temperature [4]. Subsequently, the mechanical properties of the matrix and the GFRP can change significantly vs. temperature, particularly in the transition zone or close to it. The glass transition temperature and other characteristic temperatures are different for each thermoplastic or thermosetting polymer. In footbridges, thermosets significantly below the glass transition temperature are mostly used.

The manufacture of GFRP laminate shells in infusion technology consists of the following steps. A gelcoat layer of an 0.5 mm average thickness is put on the waxed mould surface using hand lay-up technology. The glass reinforcement, i.e. fabrics/mats, are arranged on the gelcoat layer, and then the delamination fabric and the membrane are put on. After installing the drainage channels and the encapsulation, the vacuum system is turned on. After saturation of the fabrics/mats ply sequence by the resin, the channels are sequentially closed. After curing, the membrane is removed and the delamination fabric is broken off. A topcoat layer of an average thickness of 0.5 mm is placed on the laminate surface using the hand lay-up method. The topcoat layer contains wax additives to prevent oxygen inhibition which allows for complete curing. The laminate shell structure is subjected to post-curing in heat, depending on the type of resin.

Environmental ageing is defined as a combination of humidity and UV radiation, reflecting weather conditions over a specified durability period. The material constants of each structural composite, corresponding to the assumed material model, should be identified experimentally at least for the new (virgin, unaged, as-manufactured) material and the aged (after accelerated ageing) material, at room temperature (RT), as well as at the minimum and maximum service temperature levels.

Based on the literature review (not presented in this paper), to date the impacts of temperature and/or hygrothermal ageing on selected mechanical properties of selected FRP composites, i.e. glass/polyester, carbon/epoxy, glass/epoxy, glass/aramid/epoxy laminates of specified ply sequences, have been tested on different composite specimens under various stress states, in different temperature and time ranges. The longest ageing period lasted 285 days.

It is well known that the mechanical properties of polymer composites depend on many factors, including the matrix type, reinforcement type, manufacturing technology, fibre volume fraction, operating temperature, environmental ageing, additives, and protective layers. To date, researchers have developed many approximate formulae to predict the effective material constants of a composite (a lamina) after homogenization, e.g. [4, 5]. In this paper, the selected glass-vinyl ester composite, manufactured using infusion technology, is applied. The mechanical properties of this composite were determined experimentally in set ageing-temperature regimes, in accordance with relevant standards but with some extensions and with a complementary test.

The study considers a GFRP composite box beam reflecting, on a 1:2 scale, the central part of the superstructure of the GFRP composite 5-box footbridge presented in [2]. The beam is composed of two laminate shells combined with glue on contact strips. The shells are glass-vinyl ester laminates, protected with gelcoat and topcoat coatings, respectively, excluding the contact strips. After homogenization, a single lamina (reinforced with one fabric) is modelled as a linearly elastic-brittle orthotropic material. Identification of the material constants of a single lamina is carried out for the new composite and for the aged composite after accelerated 5-year environmental ageing corresponding to the atmospheric conditions in Poland, at three service (for footbridges) temperatures, i.e. –20, 20, 55°C. The identification tests include all the elasticity and strength constants in reference to the assumed material model.

The study presents the numerical modelling and simulation of the static three-point bending test of the new and aged box beam, at three service temperatures. The modelling and simulation were validated in a previous paper by the authors, based on the experimental three-point bending test of a new beam at the temperature of 20°C [6]. Comparative studies were performed in order to determine the effects of the service temperature and the 5-year environmental ageing on the load capacity of the GFRP composite box beam.

MATERIAL SPECIFICATION AND EXPERIMENTAL TESTS PROGRAMME

The experimental identification tests concern a GFRP composite, denoted with the code BG/F, which is a layer of laminates made of the following components: an E-glass, bi-directional, quasi-balanced, stitched fabric of 800 g/m^2 weight (BAT800 and GBX800 fabrics; producer DIPEX Co., Slovakia) and a flame retardant vinylester resin (BÜFA®Firestop S 440 resin; producer BÜFA Gelcoat Plus Co., Germany). The matrix is a moderately reactive resin on a bisphenol A epoxide base, dissolved in styrene, pre-accelerated and formulated with a liquid flame retardant. The resin can be used for producing especially high quality moulded parts. Laminates based on this resin have excellent heat resistance (HDT = 90°C) and are highly resistant to dynamic loads [7]. The glass transition temperature for this resin is greater than 110°C.

According to the producer's instructions, the selected resin needs for post-curing in heat to complete the polymerization process and to achieve the respective HDT temperature. The following post-curing cycle, recommended by the producer, was employed:

- heat from RT to 60°C, at temperature rate of 0.33 K/min
- dwell at 60°C for 5 hours
- heat from 60°C to 80°C, at temperature rate of 0.16 K/min
- dwell at 80°C for a period of 1 h/1 mm of laminate thickness plus 3 h
- cool from 80°C to RT at temperature rate of 0.33 K/min.

The pre-manufactured BG/F composite plates, used to produce laminate specimens with a $[0/90]_{2S}$ or $[45/-45]_{2S}$ ply sequence, were manufactured using infusion technology and post-cured in heat. The specimens subjected to environmental ageing were covered with a 300 μm thick gelcoat (BÜFA®Firestop S250-SV, producer: BÜFA Gelcoat Plus Co., Germany). After completion of the ageing process, the gelcoat layer was abraded.

The environmental ageing programme was developed according to [8]. Ageing of the gelcoat-protected composite plates was conducted under the following conditions: (a) chamber temperature of 35°C, (b) intensity of UV radiation of 340 nm wavelength was equal to 1.33 W/m^2, (c) exposure period of 5 months equivalent to accelerated 5-year environmental ageing.

The complete ageing cycle consists of three stages, each appropriately divided into light and dark cycles and dry and wet periods defined by relative humidity (RH). The first stage is light (12 h, 20% RH) and dark (12 h). The dark cycle is divided into two periods: dry (6 h, 20% RH) and wet (6 h, ~100% RH). The total testing time is 1224 h, including an irradiation time of 612 h. The absorbed UV radiation dose is 7.32 MJ/m^2. The second stage is light (16 h) and dark (8 h, 20% RH). The light cycle is divided into two periods: dry (8 h, 10% RH) and wet (8 h, ~100% RH). The total testing time is 1224 h, including an irradiation time of 816 h. The absorbed UV radiation dose at this stage is 4.88 MJ/m^2. The third stage is light (8 h) and dark (16 h). The light cycle is divided into two periods: dry (4 h, 20% RH) and wet (4 h, ~100% RH). The dark cycle is also divided into two periods: dry (8 h, 20% RH) and wet (8 h, ~100% RH). The total testing time is 1224 h, including an irradiation time of 408 h. The absorbed UV radiation dose is 2.44 MJ/m^2 [8].

The environmental ageing of the gelcoat-protected BG/F composite, according to the above specified ageing programme, was performed using an Atlas Ci 3000+ Xenon ageing chamber, at the Centre for Materials Research and Mechatronics, Motor Transport Institute, Warsaw, Poland. The apparatus is equipped with a basket to attach 20 plates with a total exposure area of 2000 cm^2.

With respect to GFRP composite footbridges, the manufacturing temperature equals 20°C and the design temperature range is [–20°C, 55°C]. The identification tests were carried out using new BG/F composite samples (code N) and aged BG/F composite samples (code A), at three temperatures: –20, 20, 55°C. The codes of the performed tests are N/–20, N/20, N/55, A/–20, A/20, A/55, respectively. The identification tests were carried out at the Laboratory of Strength of Materials and Structures, Department of Mechanics and Applied Computer Science, Faculty of Mechanical Engineering, Military University of Technology, Warsaw, Poland.

MATERIAL MODEL AND RULES FOR IDENTIFYING MATERIAL CONSTANTS

After homogenization, the BG/F composite is modelled as a linearly elastic-brittle orthotropic material. The material directions are: 1 - 0° fibre direction (warp), 2 - 90° fibre direction (weft), 3 - thickness direction. The components of the stress and strain tensors in the local material axes of the homogenized medium are denoted as σ_1, σ_2, σ_3 - normal stresses, τ_{12}, τ_{23}, τ_{31} - shear stresses, ε_1, ε_2, ε_3 - normal strains, γ_{12}, γ_{23}, γ_{31} - shear strains. The material is described by 9 effective elastic constants and 9 effective strength constants (expressed in stresses), in the material directions or planes, i.e. E_1, E_2, E_3 - Young's moduli, ν_{12}, ν_{13}, ν_{23} - Poisson's ratios, G_{12}, G_{13}, G_{23} - shear moduli, R_{1t}, R_{2t}, R_{3t} - tensile strengths, R_{1c}, R_{2c}, R_{3c} - compressive strengths, R_{12}, R_{13}, R_{23} - shear strengths. The Poisson's ratios meet the well-known conditions, i.e. [4]

$$\frac{\nu_{ij}}{E_i}=\frac{\nu_{ji}}{E_j},\quad i,j=1,2,3,\quad i\neq j \tag{1}$$

The material constants are determined based on the following tests: tension in direction 1 (code TT1), compression in direction 1 (code TC1), compression in

direction 3 (code TC3), shear in plane 12 (code TS12), shear in plane 13 (code TS13). Material symmetry conditions are used to complete the material constants set. Tests TT1, TC1, TS12, TS13 are conducted in accordance with the relevant EN ISO standards [9-13]. The TS13 test is extended compared to [12], via incorporating separation of the bending and shear displacements. Shear strength R_{13} includes delamination. The TC3 test is not standardized. The experimental identification tests allow determining most of the elastic and strength constants of the orthotropic material under consideration (Table 1). The missing material constants are determined from the conditions put on linearly elastic–brittle orthotropic materials [4]. Subscripts *t, c* denote tension and compression, respectively.

The compression test in direction 3 is designed based on the compression test in direction 1. The TC3 test was performed on cuboids manufactured by bonding, with very thin adhesive layers, three square laminate plates of a ply sequence $[0/90]_{2S}$ each, of dimensions $b \times b$ = 10×10 mm. 06-060LZ-EA-120 Vishay strain gauges were applied in pairs on two opposite faces, in directions 1 and 3. The experiment was conducted at the crosshead speed of 1 mm/min. Identification is performed based on charts $\sigma_3(\varepsilon_3)$, $v_{31}(\varepsilon_3)$ and the following formulae:

$$\sigma_3 = \frac{F}{b^2}, \quad R_{3c} = \frac{F_{\max}}{b^2} \tag{2}$$

where: F - compression force, F_{max} - maximum load value at failure. The E_{3c} modulus is determined on the basis of the initial quasi-linear section of the graph, using linear interpolation. The v_{31c} ratio is determined on the basis of the graph $v_{31c}(\varepsilon_3)$ as the arithmetic mean value, excluding the ill-conditioned edge section.

TABLE 1. **Strength tests to determine material constants of orthotropic composite**

TABELA 1. **Próby wytrzymałościowe do wyznaczenia stałych materiałowych kompozytu ortotropowego**

Test code	Strength test	Identified constants
TT1	tensile test in direction 1 [9]	E_{1t}, v_{12t}, R_{1t}
TC1	compressive test in direction 1 [10]	E_{1c}, R_{1c}
TC3	compressive test in direction 3 (not standardized)	E_{3c}, v_{31c}, R_{3c}
TS12	shear test in plane 12 through tension ($[45/-45]_{2S}$ ply sequence) [11]	G_{12}, R_{12}
TS13	interlaminar shear test in plane 13 ([12], with extension)	G_{13}, R_{13}

The TS13 interlaminar shear test is similar to the 3-point bending mode except that a lower length to thickness ratio increases the shear stress compared to the longitudinal normal stress in order to achieve failure due to interlaminar shear. The standard specimen has dimensions $l \times b$ = 20×10 mm, where: l - total length, b - specimen width [12]. The dimensions may be modified to $l = 10h$, $b = 5h$ where h - sample thickness. The following dimensions are assumed: l = 26 mm, b = 13 mm, L = 20 mm, h = 2.6 mm. The test was done at the crosshead speed of 1 mm/min. Partially non-standardized calculations are based on charts $F(s)$, $s_M(s)$, $s_T(s)$, $\tau_{13}(\gamma_{13})$, where F - stamp pressure force, s - vertical displacement of the crosshead, s_M, s_T - vertical displacement at the sample midspan due to bending and shear, respectively. The calculations based on the classical strength of materials are as follow (Fig. 1):

$$s_M(s) = \frac{F(s)L^3}{4E_1 bh^3}, \quad s_T(s) = s - s_M(s)$$
$$\gamma_{13}(s) = \frac{3s_T(s)}{L}, \quad \tau_{13}(s) = \frac{3F(s)}{4bh} \tag{3}$$

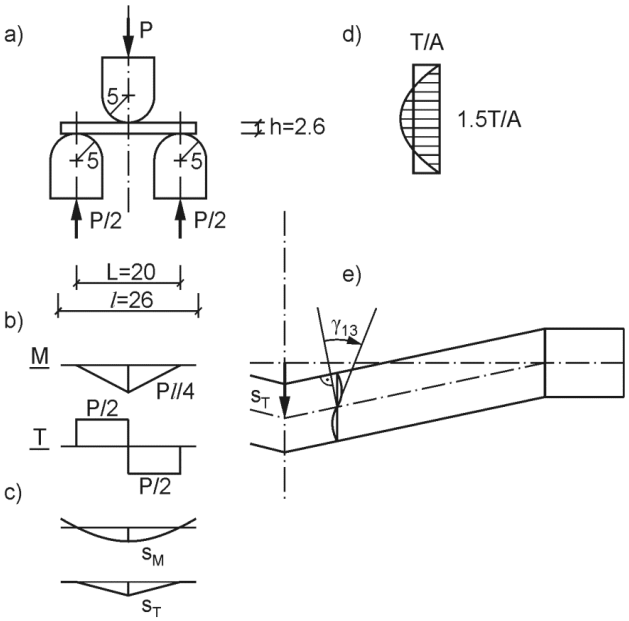

Fig. 1. Three-point bending used in TS13 test: a) schematic instrumentation; b) bending moment and shear force graphs; c) graphs of displacements induced by bending and shear; d) distribution of shear stresses on cross-section height; e) cross section distortion

Rys. 1. Zginanie 3-punktowe zastosowane w teście TS13: a) schemat oprzyrządowania; b) wykresy momentu zginającego i siły tnącej; c) wykresy przemieszczeń wywołanych zginaniem i ścinaniem; d) rozkład naprężeń stycznych na wysokości przekroju poprzecznego; e) deplanacja przekroju poprzecznego

Equations (3) allow one to determine the approximate graph $\tau_{13}(\gamma_{13})$. The shear module is calculated as

$$G_{13} = \frac{\tau''_{13} - \tau'_{13}}{\gamma''_{13} - \gamma'_{13}} \tag{4}$$

where $\tau'_{13}, \tau''_{13}, \gamma'_{13}, \gamma''_{13}$ - stresses and strains corresponding to linear regression of the graph $\tau_{13}(\gamma_{13})$, excluding the ill-conditioned edge section. The shear strength is equal to

$$R_{13} = \frac{3F_{\max}}{4bh} \tag{5}$$

where F_{max} - maximum load at sample rupture.

The identification results were processed statistically according to [13], based on normal distributions of the output quantities. The tests were performed on 5 specimens each for the new material and on 3 specimens each for the aged material.

MATERIAL CONSTANTS IDENTIFICATION RESULTS

After accelerated 5-year ageing of the BG/F composite plates coated with a 300 μm thick gelcoat layer, checking the state of the surface topography was performed using the optical profilometry method. The tested area was a rectangle of dimensions 10×2 mm. The tests included both surfaces of the aged sample, i.e. the radiation exposed front surface and the back surface. The measurements were carried out at the Motor Transport Institute, Warsaw, Poland using the non-contact optical profilometer Contour GT-K1. Analysis of the topography of the surface exposed to UV radiation indicated the presence of cavities with a depth not exceeding 30 μm, which has a small effect on reducing protection.

The identification results refer to a single lamina reinforced with the BAT800 [0/90] fabric. The basic parameters of samples with the $[0/90]_{2S}$ ply sequence are as follow: average density 1.71 g/cm^3, average thickness of one layer 2.65/4 = 0.663 mm, average fibre mass fraction 71%. The standardized and non-standardized tests were performed using the universal testing machine INSTRON 8802, without the use of a heat chamber (at 20°C), using the heat chamber (at 55°C) and using the heat chamber with liquid CO_2 (at −20°C).

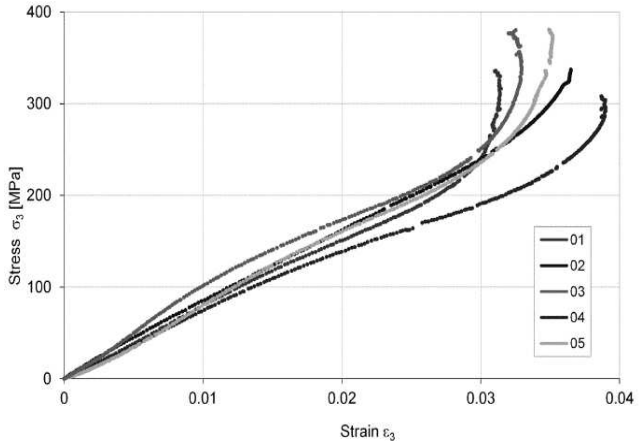

Fig. 2. $\sigma_3(\varepsilon_3)$ chart obtained in TC3 test of BG/F composite samples, under N/20 conditions

Rys. 2. Wykresy $\sigma_3(\varepsilon_3)$ otrzymane w teście TC3 próbek kompozytowych BG/F w warunkach N/20

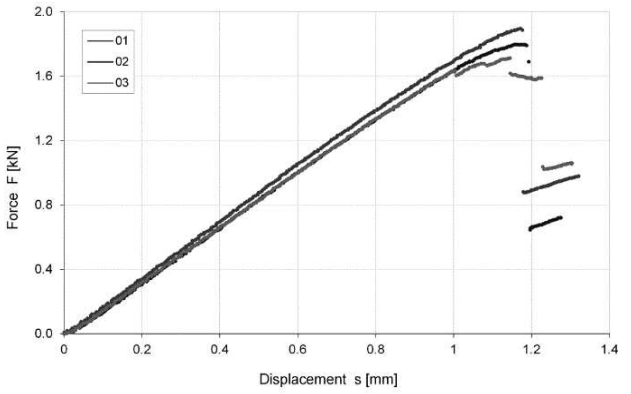

Fig. 3. $F(s)$ chart obtained in TS13 test of BG/F composite samples, under A/–20 conditions

Rys. 3. Wykresy $F(s)$ otrzymane w teście TS13 próbek kompozytowych BG/F w warunkach A/–20

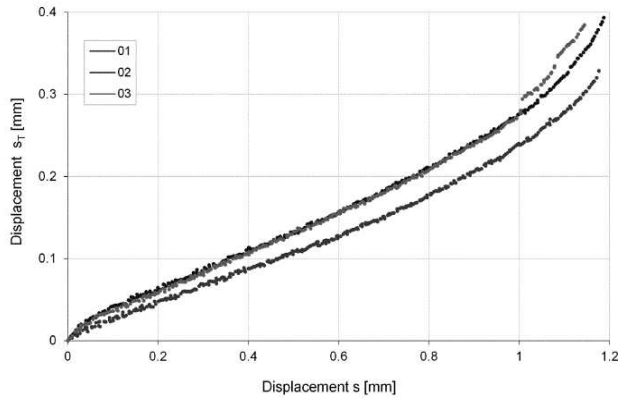

Fig. 4. $s_T(s)$ chart obtained in TS13 test of BG/F composite samples, under A/–20 conditions

Rys. 4. Wykresy $s_T(s)$ otrzymane w teście TS13 próbek kompozytowych BG/F w warunkach A/–20

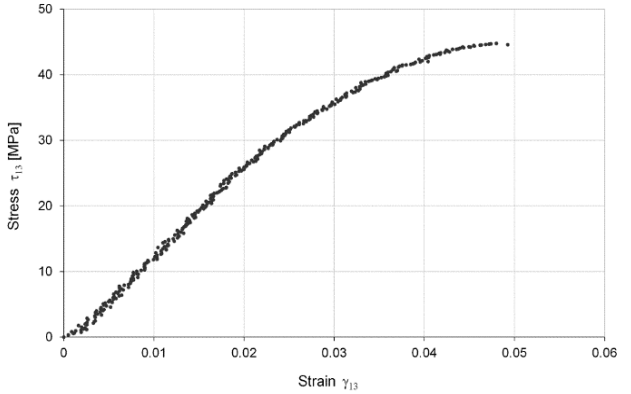

Fig. 5. $\tau_{13}(\gamma_{13})$ chart for sample 01 in TS13 test of BG/F composite, under N/–20 conditions

Rys. 5. Wykres $\tau_{13}(\gamma_{13})$ dla próbki 01 w teście TS13 kompozytu BG/F w warunkach N/–20

The representative experimental curves, obtained according to the identification methodology developed in Section Material model and rules for identifying material constants, are presented in Figures 2-5. The analogous diagrams in the remaining ageing-temperature conditions are qualitatively consistent with these

graphs. The ageing-temperature conditions considered in this study result in more than 300 final curves or curve sections. In total, the identification experiments and processing of the measurement results took one year approximately. The values of the material constants describing the BG/F composite are summarized in Tables 2, 3.

TABLE 2. **Elastic constants of new and 5-year aged BG/F composite**

TABELA 2. **Stałe sprężystości kompozytu BG/F nowego i poddanego starzeniu 5-letniemu**

Constant	Unit	N/–20	N/20	N/55	A/–20	A/20	A/55
$E_1 = E_2$	GPa	31.6	23.4	32.3	19.8	23.9	23.2
E_3	GPa	16.2	7.78	13.1	10.9	8.32	4.44
$v_{12} = v_{21}$	–	0.083	0.153	0.116	0.123	0.103	0.109
$v_{31} = v_{32}$	–	0.210	0.197	0.151	0.106	0.147	0.079
$v_{13} = v_{23}$	–	0.410	0.593	0.372	0.193	0.422	0.413
G_{12}	GPa	4.56	3.52	2.43	4.59	3.69	2.65
$G_{13} = G_{23}$	GPa	2.35	1.36	1.14	1.20	0.90	0.781

TABLE 3. **Strength constants of new and 5-year aged BG/F composite**

TABELA 3. **Stałe wytrzymałości kompozytu BG/F nowego i poddanego starzeniu 5-letniemu**

Constant	Unit	NS/–20	NS/20	NS/55	AS/–20	AS/20	AS/55
$R_{1t} = R_{2t}$	MPa	557	449	528	465	428	421
R_{3t}	MPa	95	95	95	95	95	95
$R_{1c} = R_{2c}$	MPa	497	336	351	365	334	260
R_{3c}	MPa	422	348	365	431	337	329
R_{12}	MPa	56.9	45.2	30.9	59.1	47.1	31.1
$R_{13} = R_{23}$	MPa	38.7	34.7	35.9	42.4	36.7	27.5

DESCRIPTION OF GFRP COMPOSITE BOX BEAM UNDER THREE-POINT BENDING TEST

The BG/F composite box beam and the experimental instrumentation for the 3-point bending test with kinematic excitation were presented in a previous paper [6], with analysis focused on the FE (finite element) mesh size and experimental validation of the numerical modelling and simulation, under N/20 conditions. The cross-section of the beam is presented in Figure 6.

The overall dimensions of the beam are equal to 2350×600×258 mm. The beam is composed of a hat shaped top composite shell (TS) and a flat bottom composite shell (BS) glued together at the flat contact surface using a 0.5 mm thick NORPOL FI-184 adhesive layer. The shells have the thickness of 4.00 mm (without protective layers).

The ply sequence for the TS and BS laminates is $[BAT/GBX/BAT]_2 = [0/45/0]_2$, wherein only the fabric warp orientation is reflected. The following interpretation of angles is assumed: 0/90 - directions parallel and perpendicular to the beam axis (warp and weft directions in BAT800 fabric), 45/–45 - directions at 45°/–45° to the beam axis (warp and weft directions in GBX800 fabric). In this study, part of the material constants (G_{13}, R_{13}) has been corrected compared with the data in [6].

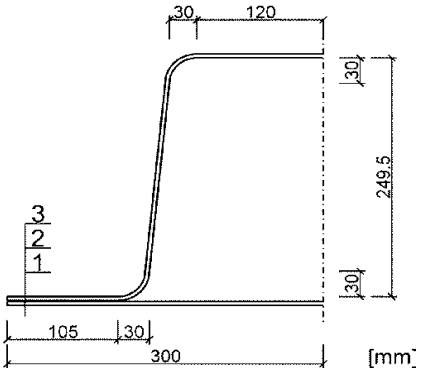

Fig. 6. Cross-section of BG/F composite box beam: 1 - bottom shell BS (4 mm), 2 - adhesive layer (0.5 mm), 3 - top shell TS (4 mm)

Rys. 6. Przekrój poprzeczny belki skrzynkowej z kompozytu BG/F: 1 - powłoka dolna BS (4 mm), 2 - warstwa kleju (0,5 mm), 3 - powłoka górna TS (4 mm)

NUMERICAL MODELLING OF THREE-POINT BENDING TEST OF THIN-WALLED BOX BEAM

The finite element (FE) numerical model of the beam was developed in HyperMesh v12.0 software, based on the geometrical model created in the Catia v5r19 system, using the following tools: *Generative Shape Design* (surface modelling), *Part Design* (solid modelling), and *Assembly Design* (assembly performance). The geometric and material properties, contact, loads and type of analysis were defined in the MSC.Marc 2010 system [14]. In this study, the original names of the finite elements, parameters and options in the MSC.Marc 2010 system are applied. The chosen finite elements, parameters and options are described in a concise manner at the first references.

The numerical model of the box beam is shown in Figure 7. Only QUAD4 shell FEs are used for the meshing. The basic size of the FEs is 20×20 mm. This size was reduced to approximately 12×12 mm in the stamp impact zone and the chamfered areas. The adhesive layer is treated as one of the laminate layers. The total numbers of FEs and nodes of the box beam model are 10836 and 10922, respectively. The steel supports and the moving steel stamp are modelled as surfaces with perfectly rigid body properties.

Laminate FEs are in *Bilinear Thick-Shell* (No. 75) formulation [14]. It is a bilinear, 2-dimensional, 4-node shell finite element having three translational and three rotational degrees of freedom at each node. The transverse shear strains are calculated at the middle of the edges and interpolated to the integration points. The appropriate thickness of the shell and corresponding offsets from the mid-surfaces are defined in the geometrical properties of the FEs.

An orthotropic linearly elastic-brittle material model was applied for the laminas and an isotropic linearly elastic-brittle material model was used with respect to the adhesive. The effective material constants of the new and 5-year aged BG/F lamina, at three temperatures, are collected in Tables 2 and 3, where N/20 are the reference conditions. The material constants of the NORPOL FI-184 adhesive, based on the manufacturer's material card are equal to: E = 3100 MPa - Young's modulus, v = 0.36 - Poisson's ratio, R_t = 35.0 MPa - tensile strength, R_c = 35.0 MPa - compressive strength, S = 20.3 MPa - shear strength.

Based on the numerical and experimental identification and validation studies [15], the following failure hypotheses in the MSC.Marc system [14] have been selected: Hashin Fabric for BG/F layers and Max Stress for the glue layer. The Hashin Fabric hypothesis defines six failure indices in each integration point [14]. Each failure index defines the respective effort index calculated as $R_i = \sqrt{F_i}$, $i = 1,2,...,6$. The effort indices state the direct measure of the laminate effort. In reference to the shell model developed in the study, only indices R_1, R_2, R_3, R_4 are valid. The Max Stress hypothesis also defines six failure indices [14]. The effort indices are equal to the failure indices, i.e. $R_i = F_i$, $i = 1,2,...,6$.

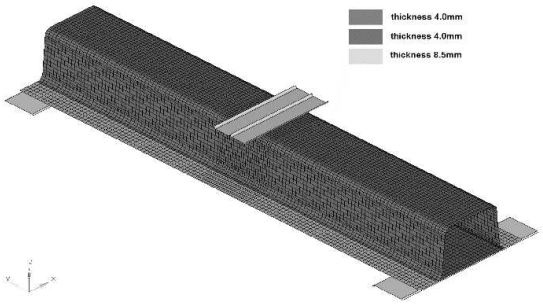

Fig. 7. FE model of BG/F composite box beam in isometric view

Rys. 7. Model numeryczny belki skrzynkowej z kompozytu BG/F w widoku izometrycznym

The *Selective Gradual Degradation* model of progressive failure was used with respect to the laminate shells [14]. This model decreases the material constants when failure occurs. Within an increment, it attempts to keep the highest failure index less than or equal to 1. Whenever a failure index larger than 1 occurs, the stiffness reduction factor is calculated based upon the value of the failure index.

Possible steel-laminate friction pairs were declared in respective subareas of potential contact of the system parts. The *Segment-to-Segment* contact model with the *Touching* option, including the Coulomb friction model, was applied [14]. The steel-laminate friction coefficient at high pressure, $\mu = 0.14$, was determined from the authors' experiments. The *Gravity Load* option was taken into account.

Theoretically, the system for the three-point bending test is perfectly bisymmetric. Before applying the vertical load via kinematic excitation, the model is geometrically unstable (horizontal displacements at the supports are possible). In order to ensure geometrical stability of the FE model, respective translational degrees of freedom in the longitudinal and transverse symmetry planes are fixed. The rotational degrees of freedom are kept since the simulations are carried out with respect to the full numerical model.

The full Newton-Raphson method with the residual convergence criterion (relative tolerance of 0.2) is used to solve the problem. A conventional loading time of 1 s and a constant time step of 0.001 s are applied. Small strains and large rotations are taken into consideration.

EFFECTS OF SERVICE TEMPERATURE AND 5-YEAR AGEING ON LOAD CAPACITY OF COMPOSITE BOX BEAM

Figures 8 and 9 show the $F(s)$ graph for the analysed systems. Table 4 summarizes the values of $F_{\max}$ and $s(F_{\max})$ at the load capacity point of the box beam.

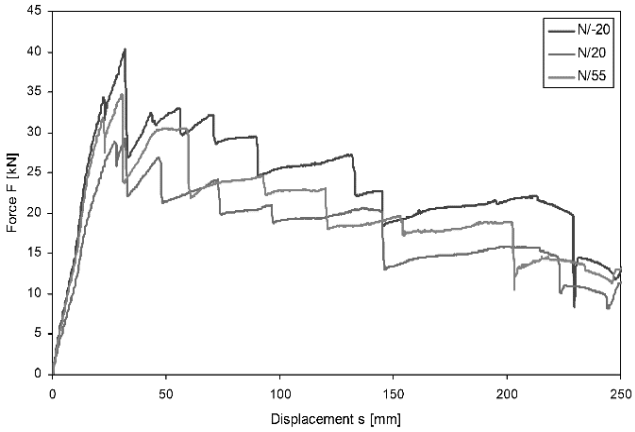

Fig. 8. $F(s)$ graph for virtual conditions N/–20, N/20, N/55

Rys. 8. Wykresy $F(s)$ odpowiadające warunkom wirtualnym N/–20, N/20, N/55

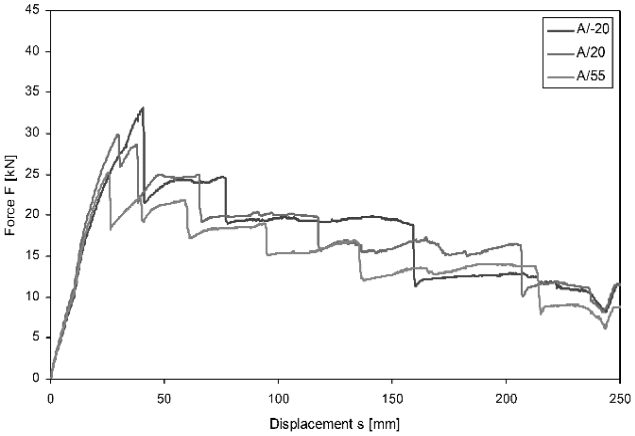

Fig. 9. $F(s)$ graph for virtual conditions A/–20, A/20, A/55

Rys. 9. Wykresy $F(s)$ odpowiadające warunkom wirtualnym A/–20, A/20, A/55

TABLE 4. **Comparison of F_{max} and $s(F_{max})$ values at load capacity point of box beam**
TABELA 4. **Porównanie wartości F_{max} oraz $s(F_{max})$ w punkcie nośności belki skrzynkowej**

Quantity	Conditions					
	N/–20	N/20	N/55	A/–20	A/20	A/55
F_{max} [kN]	40.4	29.2	34.7	33.1	29.9	25.3
$s(F_{max})$ [mm]	32.2	32.2	30.6	40.7	29.7	25.3

Taking into account the graphs presented in Figures 8, 9 and the results collected in Table 4, the following conclusions can be formulated:

1. The $F(s)$ charts corresponding to the new and 5-year aged laminates are qualitatively similar at the analysed operating temperatures. Ageing causes a significant reduction in the load capacity at the low and elevated temperatures. The load capacity of the aged and new beams at room temperature does not change.
2. Compared to the reference conditions of N/20, the load capacity of the new beam is increased by 38.4% at the low temperature (–20°C) and by 18.8% at the elevated temperature (55°C). It is the advantage of the resin used as the matrix in the BG/F composite.
3. Compared to the reference conditions of N/20, the load capacity of the 5-year aged beam increases by 13.4% at the low temperature and decreases by 13.4% at the elevated temperature. A further decrease in the load capacity is expected with increasing the durability (over five years) of the structure made of composite BG/F.
4. The values of crosshead displacement s, corresponding to the load capacity point of the box beam in the specified conditions, are similar to each other. Compared with the reference conditions, the biggest differences are for the aged beam at the low temperature (by 26.4%) and at the elevated temperature (by –21.4%).
5. Reducing the load capacity of the aged beam at the elevated temperature and increasing the vertical deflection at the midspan of the aged beam at the low temperature should be taken into account in the design of composite footbridges.

CONCLUSIONS

The study develops a methodology to identify the elasticity and strength constants of a GFRP composite modelled as an orthotropic linearly elastic-brittle material. The four standardized tests have been extended and completed with a compression test in the thickness direction. Linearly elastic behaviour of the BG/F composite was confirmed in a wide range of strains. Small non-linear effects occur prior to brittle destruction of the composite in strength tests TT1, TC1, TC3 and TS13. Substantial non-linear effects are visible in the TS12 shear test realized by stretching at an angle of ±45° relative to the fibre directions.

The impact of the 5-year environmental ageing and service temperature in the interval [–20°C, 55°C] on the elastic and strength constants of the BG/F E-glass/vinylester composite can be significant and different for particular constants. In general, after accelerated 5-year ageing, there are drops by up to 60% in the material constant values depending on the material constant and the temperature. Some material constants of the BG/F virgin material can be greater at the low or elevated temperature compared to the reference values corresponding to room temperature.

The effects of the service temperature and 5-year environmental ageing were tested for the thin-walled box beam made of the BG/F composite. A reduction in the load capacity of the aged beam at the elevated temperature (55°C) and increased deflection of the aged beam at the low temperature (–20°C) are observed. Both environmental ageing and operating temperatures should be taken into consideration in the design of composite footbridges made of BG/F laminates.

Acknowledgments

The study was supported by the National Centre for Research and Development, Poland, as a part of research project No. PBS1/B2/6/2013 (acronym FOBRIDGE), realized in the period 2013-2015. This support is gratefully acknowledged. The authors would like to express many thanks to Mr Roman Romanowski (ROMA Ltd company, Grabowiec, Poland) for the given know-how in reference to polymer composites technologies, to Dr. Pawel Gotowicki and Dr. Andrzej Kiczko (Military University of Technology, Warsaw, Poland) for conducting the experimental tests and to Dr. Dariusz Rudnik (Motor Transport Institute, Warsaw Poland) for carrying out the composite ageing and checking the state of the laminate surface topography.

REFERENCES

[1] Chroscielewski J., Klasztorny M., Miskiewicz M., Romanowski R., Wilde K., Innovative design of GFRP sandwich footbridge, Int. Conf. Footbridges: Past, Present & Future FOOTBRIDGE-2014, 16-18 July 2014, London, England, CD Conf. Proc., Paper #1250, 1-8.

[2] Klasztorny M., Chroscielewski J., Szurgott P., Romanowski R., Design and numerical testing of 5-box GFRP shell footbridge, Int. Conf. Footbridges: Past, Present & Future FOOTBRIDGE-2014, 16-18 July 2014, London, England, CD Conf. Proc., Paper #1094, 1-8.

[3] PN-EN 13121-3+A1:2010E, Ground containers made of plastics reinforced with glass fibre. Part 3. Design and production control [in Polish].

[4] Jones R.M., Mechanics of Composite Materials, Taylor & Francis, 2nd ed., London 1999.

[5] Structural Design of Polymer Composites. EUROCOMP Design Code and Handbook, Ed., J.L. Clarke, The European Structural Polymeric Composites Group, E & FN SPON, An Imprint of Chapman & Hall, London 1996.

[6] Klasztorny M., Nycz D., Cedrowski M., Modelling, simulation and validation of bending test of box segment formed as two composite shells glued together, Composites Theory and Practice 2015, 15, 2, 88-94.

[7] BÜFA®-FIRESTOP S 440 pre-accelerated VE-FR injection resin. Technical data sheet, BÜFA Gecoat Plus Co., Germany, 2013.

[8] SAE J1960. Accelerated Exposure of Automotive Exterior Materials Using a Controlled Irradiance Water-Cooled Xenon Arc Apparatus.

[9] PN-EN ISO 527-4:2000. Determination of mechanical properties at static tension. Test conditions for isotropic and orthotropic fibre-reinforced plastic composites [in Polish].

[10] PN-EN ISO 14126:2002. Fibre-reinforced plastic composites. Determination of properties at in-plane compression [in Polish].

[11] PN-EN ISO 14129:1997. Fibre-reinforced plastic composites. Determination of shear stress and corresponding strain, shear modulus and ±45° tensile strength [in Polish].

[12] PN-EN ISO 14130:2001. Fibre-reinforced plastic composites. Determination of nominal interlaminar shear strength by short beam method [in Polish].

[13] PN-ISO 2602:1994. Statistical interpretation of test results. Estimation of average value. Confidence interval [in Polish].

[14] MSC.Marc r1, Vol. A, Theory and User Information, MSC.Software Co., Santa Ana, CA, USA, 2008.

[15] Klasztorny M., Bondyra A., Szurgott P., Nycz D., Numerical modelling of GFRP laminates with MSC.Marc system and experimental validation, Computational Material Science 2012, 64, 151-156.

